Investigation of Water Vapor Permeability and Antimicrobial Property of Zinc Oxide Nanoparticles-Loaded Chitosan-Based Edible Film

S. K. Bajpai,[1] Navin Chand,[2] Varsha Chaurasia[1]

[1]*Polymer Research Laboratory, Department of Chemistry, Govt. Model Science College (Auton.), Jabalpur, MP 482009, India*
[2]*Polymer Composite Group, Advanced Materials and Process Research Institute (Formely RRL Bhopal), CSIR, Bhopal MP, India*

Received 16 December 2008; accepted 5 April 2009
DOI 10.1002/app.30550
Published online 10 September 2009 in Wiley InterScience (www.interscience.wiley.com).

ABSTRACT: This study is focused on the investigation of moisture uptake properties of chitosan films. The GAB isotherm model is found to fit well to the experimental moisture uptake data obtained at 10, 25, and 37°C. The water vapor permeability is found to increase with temperature. The use of plasticizer enhances the water vapor permeability. Finally, the films have been loaded with ZnO nanoparticles and characterized by X-ray diffraction, differential scanning calorimetry, surface plasma resonance, and scanning electron microscopic analyses. The crystal size as determined using Scherrer's equation is found to be around 15 nm. The films have shown excellent antibacterial action against the model bacterium *Escherichia coli*. © 2009 Wiley Periodicals, Inc. J Appl Polym Sci 115: 674–683, 2010

Key words: chitosan film; permeability; isotherm; ZnO-nanoparticles; antibacterial action

INTRODUCTION

There has been a growing interest in the development of food packaging films that can be used for controlling the microbiological decay of perishable food products.[1–3] The water permeability of edible films is an area of deep research, because water is often the main component of a food stuff, which also contains carbohydrates, proteins, fats, and mineral salts. At particular conditions of temperature and moisture, the interactions between these constituents can cause browning and lipid oxidation, among other reactions, and can provide the appropriate conditions for microbiological growth.[4] The antimicrobial packaging films have shown great potential to control the growth of foodborn pathogens, including *Listeria monocytogenes, Escherichia coli* 0157;H7, and *Salmonella typhimurium*.[5]

Most films, used to preserve food stuff, have been produced from synthetic polymers. Nevertheless, for environmental reasons, attention has lately been focused on natural biopolymers such as polysaccharides,[6–9] proteins,[10–12] and lipids[13] or the combination of these components for the preparation of food packaging films. These films are usually loaded with antimicrobial agents who, on coming in contact with food stuff, act on food-born microorganism and inhibit their growth. These agents belong to a wide spectrum of organic/inorganic compounds,[14] essential oils,[15] bacteria-originated antibacterial protein (bacteriocins),[16] enzymes,[17] fruit extracts,[18] etc. Although, these antibacterial agents have shown great potential in inhibiting microbial growth in food stuff, the development of new resistant strains of bacteria to current antibiotics[19] has become a serious problem in public health. Therefore, the current research has been focused on the search for new bactericides that can effectively reduce the harmful effects of microorganisms. With the emergence of nanotechnology, the search for effective biocidal agents has focused on the development of nanostructure of coinage metals like silver, copper, zinc, and gold.[20] However, the high cost of silver and gold metals has limited their use as antibacterial agents on industrial basis. Therefore, currently nanoparticle metal oxides, such as ZnO, have emerged out as a new class of important materials that are increasingly being developed for use in research and health-related applications, because of their low cost, easy availability, and unique chemical and physical properties.

Recently, there have been several reports regarding the antimicrobial activity of ZnO nanoparticles.[21] It has been reported, on the basis of preliminary

Correspondence to: S. K. Bajpai (sunil.mnlbpi@gmail.com).

growth analysis, that ZnO nanoparticles have higher antibacterial effects on microorganism like *Salmonella aureus* than other metal oxide nanoparticles.[22] Similarly, Tam et al.[23] have reported antibacterial activity of ZnO nanorods prepared by hydrothermal method. ZnO exhibited fair activity against *Escherichia coli* and *Bacillus atrophaeus*, but it was considerably more effective in the later case (at 15 m*M* versus 5 m*M* concentration respectively, showing zero viable cell count). For both organisms, damage of cell wall was observed. Recently, Padmawathy and Vijayaraghavan[24] prepared ZnO nanoparticles of different sizes and characterized by scanning electron microscopy (SEM), TEM, and X-ray diffraction (XRD) analysis. It was observed that nano ZnO showed enhanced antibacterial activity as compared with bulk ZnO and that both the abrasiveness and the surface oxygen species of ZnO nanoparticles promoted the biocidal properties.

The present work involves water sorption studies of chitosan-based edible films. In addition ZnO nanoparticles have been impregnated into chitosan films followed by a novel equilibration-cum-precipitation method. The antibacterial activity of nano ZnO-loaded films have been investigated on model bacteria *E. coli*. Zinc oxide has frequently been used in food stuff. It decomposes into Zn^{2+} ions after going into human body. Wheat proteins, fortified with ZnO, have been proved to possess good Zn absorption.[25]

EXPERIMENTAL

Materials

Chitosan was obtained by deacetylation of chitin (Hi Media, Mumbai, India) in 50 wt % NaOH solution at 90°C in nitrogen atmosphere for 2 h. The chitosan flakes, so obtained, were washed with water (Millipore Milli-Q) and dried at 50°C in vacuum. The degree of deacetylation, as determined using method of Guilbal et al.,[26] was found to be 95%. The molar mass, as determined using well-known Mark-Houwink equation was found to be 1.42×10^6, thus indicating a high molecular weight chitosan. Zinc nitrate, sodium hydroxide, nutrient agar, agar- agar Type-1, and nutrient broth were also received from HiMedia laboratories, Mumbai, India. Different salts, used to prepare saturated solutions to provide desired relative humidity (RH) were received from E-Merck, Mumbai, India. Millipore water was used throughout the investigations.

Preparation of plain chitosan film

Chitosan solution (2%, w/v) was prepared by dissolving precalculated quantity of chitosan in 4% (v/v) acetic acid solution as specified by Coma et al.[27] The solution was poured in a uniform layer of 1 mm thickness onto a polypropylene plate. The optimum conditions for casting were 60°C, for 2.5 h in a drying oven at ambient RH. The dried film was peeled from the plate and stored in a dust-free chamber at 25°C.

Preparation of ZnO nanoparticles-loaded film

The ZnO nanoparticles-loaded films were prepared by carrying out in-situ precipitation of Zn(II) in the presence of NaOH. In brief, plain chitosan film was placed in 2% (w/v) aqueous solution of zinc chloride for 12 h at 30°C. The Zn(II) loaded film was transferred into 0.02*M* aqueous solution of sodium hydroxide. After 4 h, the film was taken out and kept in electric oven (Tempstar India) at 70°C for 2 h for complete conversion of $Zn(OH)_2$ into ZnO. Finally, the film was washed with water and then put in vacuum chamber till further use. The film, prepared by immersion in 2% Zn(II) solution, was designated as zinc oxide-loaded chitosan (2) [ZOLC(2)] film while plain chitosan film was named as PC film.

Film characterization

The morphological features of plain and ZnO-loaded film were observed using a JOEL JSM840A (Japan) SEM. Differential scanning calorimetric (DSC) analysis was performed with a Metter DSC-30 thermal analyzer with PC and ZOLC. Film of known weight (Ca, 2.4 mg) was taken in a sealed aluminium pans and the sample was heated from 40 to 260°C at the heating rate of 20°C/min under the constant flow of argon gas. The XRD pattern of nano ZnO was analyzed with a PANalytical X'pert PRO MPDR X-ray diffractometer. The UV–visible spectrum of the nano ZnO dispersed in distilled water was recorded in UV–visible spectrophotometer (Shimadzu 6300) in the range of 300 to 550 nm.

Moisture content studies

The moisture sorption isotherms were determined gravimetrically using the static method as described by Alhamdan and Hassan.[28] Preweighed films were placed in Petri dishes inside glass dessicators containing different saturated salt solutions, thus providing constant RH environment ranging from 3 to 98% as described elsewhere.[29] The dessicators were placed inside temperature-controlled incubators (Tempstar India), set at desired temperature. The samples were weighed at different time intervals using electronic balance (Denver, Germeny) with an accuracy of 0.0001 g. Equilibrium was considered to

have been obtained when three consecutive measurements were found to be identical. The equilibrium moisture contents were calculated on dry basis from which moisture sorption isotherms were obtained.

Water vapor permeability measurement

Water vapor transmission of film was measured using ASTM E 96-93 method.[30] The test cups were filled with 20 g of silica gel (desiccant) to produce a 0% RH below the film. A sample was placed inbetween the cups and the silicon-coated ring cover and held with four screws around the cups circumference. The air gap was at $\sim$ 1.5 inbetween the film surface and desiccant. The water vapor transmission rate (WVTR) of each film was measured at 100% RH and 25°C $\pm$ 1°C. After taking initial weight of the test cup, it was placed in glass desiccators containing distilled water to provide 100% RH. The cups were taken out at different time intervals and weighed accurately. Three replicates of each sample were measured.

The WVTR and other related parameters were calculated[31]:

$$\mathrm{WVTR} = \frac{\Delta W}{\Delta t\, A} \quad (\mathrm{g\,s^{-1}\,m^{-2}}) \tag{1}$$

$$\mathrm{Permeance} = \frac{\Delta W}{\Delta t\, A\, \Delta P} \quad (\mathrm{g\,s^{-1}\,m^{-2}\,Pa^{-1}}) \tag{2}$$

$$\mathrm{Permeability} = \frac{\Delta W\, \chi}{\Delta t\, A\, \Delta P} \quad (\mathrm{g\,s^{-1}\,m^{-1}\,Pa^{-1}}) \tag{3}$$

where $\Delta W/\Delta t$ is the amount of water gain per unit time of transfer, χ is the film thickness, A the area exposed to water surface (cm^2), and ΔP is water vapor pressure difference between both sides of the film.

Antibacterial studies

Antibacterial studies of ZOLC film were investigated quantitatively and qualitatively by the zone inhibition method,[32] killing kinetics and viable cell count method,[33] respectively, with *E. coli* as a model bacteria.

In zone inhibition method, 100 μL of the inoculum solution was added to 5 mL of the appropriate soft agar, which was overlaid onto hard agar plates. Circular discs were cut from the test films (diameter = 1.5 cm) and were placed on the bacterial lawns. The plates were incubated for 48 h at 37°C in the appropriate aerobic incubation chamber. The plates were visually examined for zones of inhibition around the film disc and the size of the zone diameter was measured at two cross-sectional points and the average was taken as the inhibition zone.

For the liquid culture test, each film was cut into squares (1 $\times$ 1 cm^2). These sample squares were immersed in 20 mL nutrient broth in a 25 mL universal bottle. The medium was inoculated with 200 μL of *E. coli* in its late exponential phase, and then transferred to an orbital shaker and rotated at 37°C at 200 rpm. The culture was sampled periodically during the incubation to obtain microbial growth profiles. The same procedure was repeated for the control plain chitosan film. The optical density was measured at 600 nm. The OD values were converted into concentrations of *E. coli* colony forming units per millliter using the approximation that an OD value of 0.1 corresponded to a concentration at 10^8 cells/mL.

Finally, in cell count method, a 100 μL sample of bacterial suspension cultured in nutrient broth (with a concentration of 10^7 colony forming units/mL of *E. coli*) was plated on definite quantity of finely cut pieces of film and the plates were incubated at 37°C. The number of resultant colonies was counted after 24 h of incubation.

All the experiments have been done in triplicate and average data have been produced.

RESULTS AND DISCUSSION

Formation of ZOLC film

Chitosan,a derivative from deacetylation of chitin, has been a well-known sorbent for metal ions such as Zn^{2+}, Ca^{2+}, Fe^{3+}, due to the presence of amine groups that serve as strong chelation sites for these metal ions.[33] On the basis of this fact, the overall formation of ZnO nanoparticles within the chitosan film may be explained as follow.

When chitosan film is immersed in aqueous solution of $ZnCl_2$, Zn(II) ions enter into the network and are firmly attached at $-NH_2$ groups present along the chitosan chains. In addition, —OH groups may also serve as additional binding sites for incoming zinc cations. When Zn^{2+} ions-loaded film is put in aqueous NaOH solution, OH^- ions also enter into the network and cause precipitation of $Zn(OH)_2$ which, on thermal curing, yield ZnO nanoparticles. In this way, the ZnO nanoparticles-loaded chitosan film is produced. Here, it is worth mentioning that $-NH_2$ and —OH groups that are present within the matrix, serve as templets for the formation of uniformaly distributed ZnO nanoparticles. Almost similar results have also been reported by us previously[34] for the in-situ formation of silver nanoparticles in the poly(acrylamide-*co*-acrylic acid) hydrogel networks.

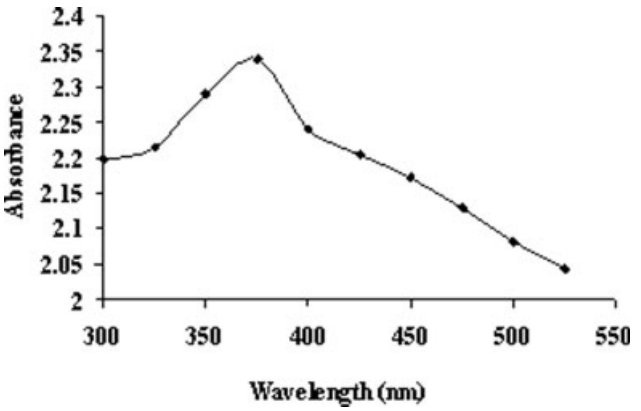

Figure 1 Surface plasmon sspectrum for ZnO nanoparticles.

Characterization of ZOLC film

The surface plasma resonance is a characteristic of metal nanostructures. In Figure 1, UV–visible spectrum of dispersion of ZnO nanoparticles has been depicted. The excitation absorption peak of ZnO particles is observed at nearly 363 nm which is fairly close to the absorption peak of 361 nm as obtained by Vigneshwaran et al.[35]

Figure 2 shows XRD pattern of nano ZOLC film. The peaks obtained at different crystal planes of nano zinc oxide were very close to reported data (JCPDS76-0704). Our values were also resembling with those obtained by Li et al.,[36] who reported 2θ values of 31.7, 34.4, 36.2, 47.5, 56.6, 62.8, and 69.1 for reflections at (100), (002), (101), (110), (103), and (112) planes. The values of 2θ as displaced in Figure 2 are 31.6, 34.4, 36.0, 47.5, 56.6, 63.0, and 69.2, respectively, which are almost identical with the reported values. In addition to this, the presence of chitosan is also confirmed by the diffraction peaks observed at $2\theta = 8.5$, 15.8, and 23.0, which also match with the values reported by Zhong and Xia.[37] Here, it is also worth mentioning that some additional small peaks observed may be due to presence of other impurities. Finally, the grain size was evaluated using the well-known Scherre's equation.

$$D = \frac{K\lambda}{(b - b_0)\cos\theta} \quad (4)$$

when, Cauchy peak type is assumed. Here, D is the crystal size, λ is the X-ray wave length, b is the width of the peak (full width at half maximum), b_0 is the instrumental peak broadening, and the Scherrer constant K is 0.89. The crystal size for (002) and (100) peaks were found to be 15.2 and 16.8 nm, thus indicating the formation of almost uniform-sized ZnO nanoparticles.

DSC analysis

Figure 3 depicts the DSC thermograms for plain and ZOLC(2) films. It was observed that the glass transition temperatures were nearly 138.8 and 140.2°C, respectively. A slight increase in T_g value is also indicative of incorporation of ZnO nanoparticles into the chitosan network, thus providing more thermal stability.

SEM analysis

Figure 4(A,B) shows the SEM images of ZOLC(1) and ZOLC(2) films, respectively. It is clear that there is dense population of ZnO nanoparticles in the film prepared with 2% $ZnCl_2$ solution. In addition, the almost uniform distribution of ZnO nanostuctures establishes the superiority of present method involving in in-situ formation of zinc oxide nanostructures within the chitosan film matrix.

GAB sorption isotherm studies

The moisture sorption isotherm of dried plain chitosan (PC) film at 10, 25, and 37°C is shown in Figure 5. It is clear that all the curves show typical sigmoidal shape thus confirming Type II classification which is characteristic of biological materials and high molecular weight sugars, which sorp relatively small amount of water at lower activity and large amount of high-relative humidities.[38] The variation in moisture content with temperature reveals some interesting results. The moisture uptake is observed to decrease when temperature is raised from 10 to 37°C. This behavior is most common for hydrated food materials, protein-based films[39] and may

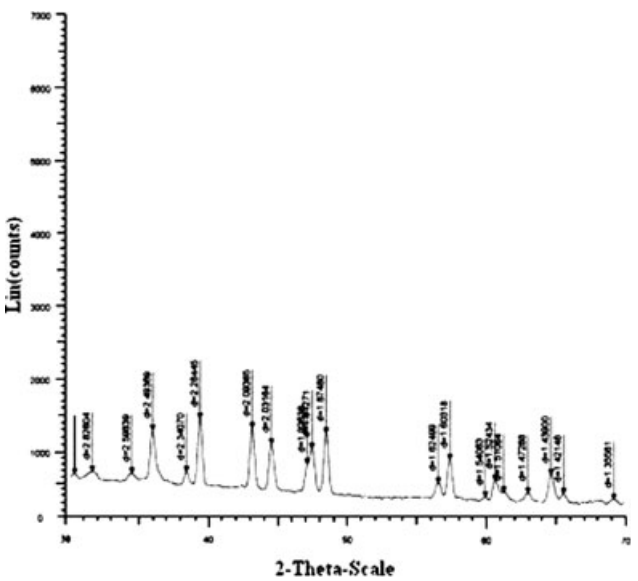

Figure 2 X-ray diffraction pattern for ZnO nanoparticles-loaded chitosan film.

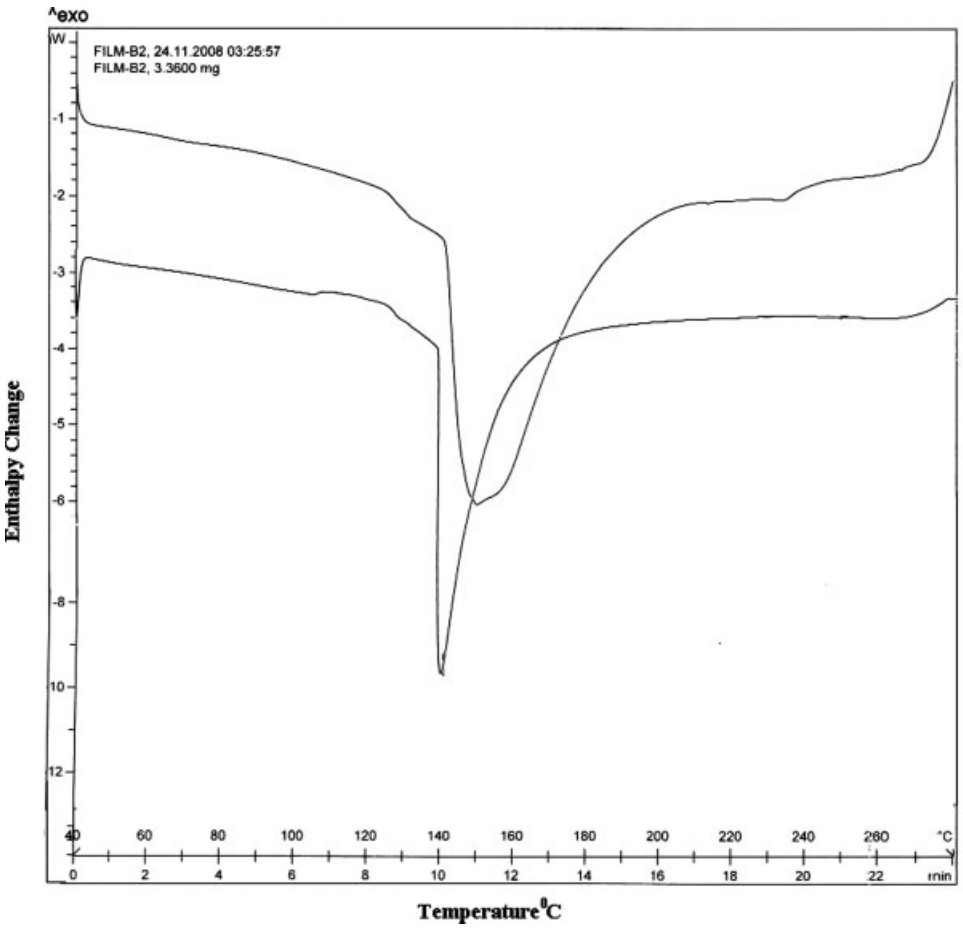

Figure 3 DSC thermograms for (A) PC and (B) ZOLC(2) films.

simply be attributed to the fact that increase in temperature causes an increase in kinetic energy of water vapor molecules and therefore van der Waals forces between sorbed water vapor molecules and chitosan film become weak, thus resulting in decrease in moisture uptake. Thus, moisture sorption may be regarded as exothermic process because moisture uptake decreases with increase in temperature. The data for moisture sorption, obtained at three temperatures, were correlated by well-known GAB sorption isotherm[40] given as

$$\frac{a_w}{W} = \frac{1 - 2Ka_w - CK^2a}{CKW_m} \tag{5}$$

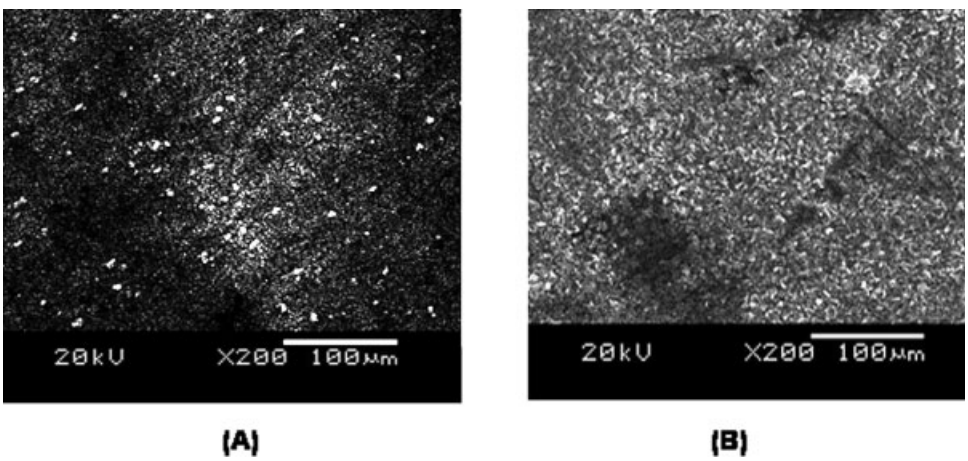

Figure 4 SEM images for (A) PC and (B) zinc oxide nanoparticles-loaded film.

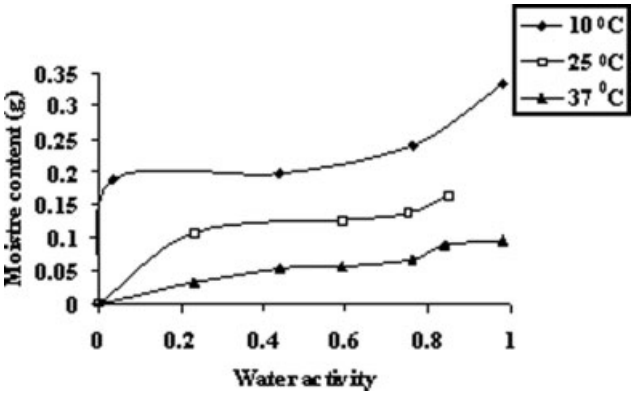

Figure 5 GAB isotherms for PC film at different temperatures.

where a_w denotes the water activity, W is the water content sorbed on 1 g of film, W_m is the water content adsorbed on the monolayer, and C and K are the sorption constants related to the temperature. Here, it is to be mentioned that the value of monolayer moisture content (W_m) is of particular interest, because it indicates the amount of water that is strongly adsorbed to specific sites at the film surface. In this study, the values of W_m, as determined using nonlinear regression analysis, were found to be 0.135, 0.075, and 0.036 g water/g dry film at 10, 25, and 37°C, respectively. These values also indicate that moisture content decreases with increase in temperature. Similar results have also been reported by Bertuzzi et al.[9] for the starch-based edible films.

Water vapor permeability studies

Water vapor permeability (WVP) is proportionality constant and is assumed to be independent of the water vapor gradient applied across the films. However, hydrophilic materials such as proteins and polysaccharides-based films deviate from this ideal behavior due to interaction of penetrating water

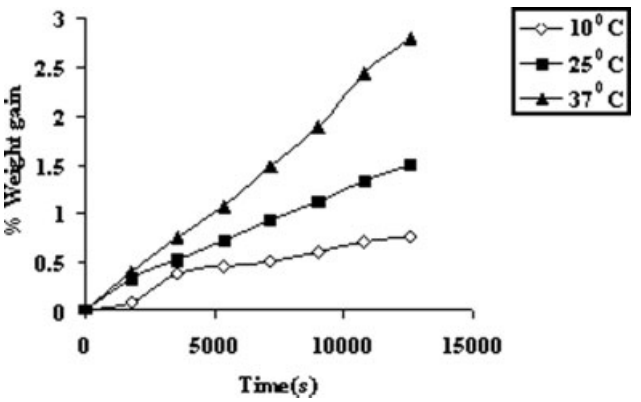

Figure 6 Kinetics of water vapor transmission through PC at different temperatures.

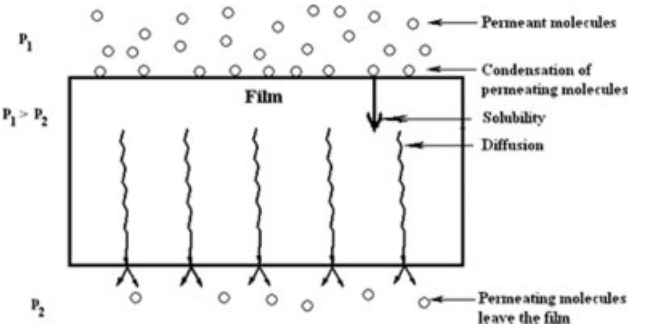

Figure 7 Scheme showing permeation of water vapors through a film.

molecules with polar groups of film constituent.[41] Because a main function of edible film is often to impede moisture transfer between food and the surrounding atmosphere, or between two components of heterogeneous food products, WVP is a significant parameter to be studied.

Figure 6 shows the dynamics of water vapor transmission through plain chitosan film at 10, 25, and 37°C. The almost linear character of the curves indicates steady-state water vapor transport and permits determination of WVTR. It is clear from Figure 6 that transmission of water vapors through film is enhanced with the increase in temperature. To explain the observed finding, it is necessary to understand the mechanism of water vapor transmission through film.[42] In Figure 7, the permeation of water vapor molecules through the film is shown. First, the permeating molecules condense on surface and solubilize into the film. This is followed by diffusion in which permeating molecules have to find their way through the film. Finally, these molecules leave the surface of the film at other side. In the light of the proposed mechanism, the observed increase in transmission of water vapor through the film may be explained. When temperature is increased, except the first step, i.e., condensation of water vapor molecules on the surface, all remaining steps are enhanced. In other words, solubility of molecules in the film, their diffusion through the film matrix and their desorption at other end undergo appreciable enhancement. Hence, the overall effect is the increase in permeability of water vapors. The various transmission parameters, as calculated using eqs. (1)–(3), have been detailed in Table I. The values of different parameters obtained at three temperatures also support our arguments.

Isosteric heat of sorption (q_{st})

The net isosteric heat of sorption, q_{st}, is a good measure of the interaction of water vapor with the solid substrate. It is also known as binding energy of sorption and defined as the difference $q_{st} - \Delta H_{vap}$,

TABLE I
Kinetics of Permeability of Plain Chitosan Film at Different Temperatures

Parameters	Temperatures		
	10°C	25°C	37°C
WVTR (g s^{-1} m^{-2})	0.122	0.175	0.350
Permeance (g s^{-1} m^{-2} Pa^{-1})	1.95×10^{-5}	2.79×10^{-5}	5.5×10^{-5}
Permeability (g s^{-1} m^{-1} Pa^{-1})	3.91×10^{-10}	5.59×10^{-10}	11.18×10^{-10}

where q_{st} is the total heat of sorption and ΔH_{vap} is heat of vapourization of water at given temperature.[43] Thus, it may be considered as an indicative of intermolecular attractive forces between the sorption sites and water vapor.

The integrated form of Clausius-Clapeyron equqtion, which correlates water activity with function of temperature, can be given as

$$\ln a_w = \frac{-q_{st}}{RT} + C \quad (6)$$

where q_{st} is the net isosteric heat of sorption (kJ mol^{-1}), R is gas constant ($R = 8.314$ kJ mol^{-1} K^{-1}), and C is a constant.

Water activity was plotted against reciprocal of absolute temperatures at various moisture contents as shown in Figure 8. The sorption isosteors showed smooth straight lines and hence confirmed that eq. (6) fitted the experimental data. For the moisture content range of 0.05–0.10, the net q_{st} values were obtained in the range of 38.20–43.40 kJ/mol. The values obtained indicate that q_{st} values are large at low moisture content and decrease with an increase in material moisture content. The observed positive values of q_{st} suggest an easy physical sorption of water molecules forming a mono molecular layer. Finally, the q_{st} values, as a function of moisture content are shown in Figure 9. It is clear that q_{st} values decrease with increase in moisture content. This may be attributed to the fact that initially sorption occurs

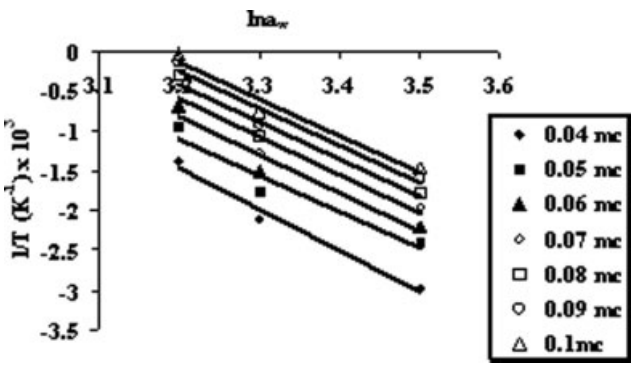

Figure 8 Water activity versus reciprocal of temperature plots for plain chitosan film to determine q_{st}.

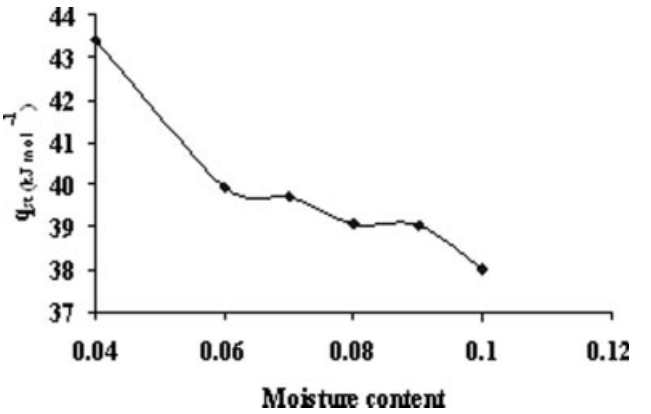

Figure 9 Variation in values of q_{st} with moisture content.

on the most active available sites, thus giving rise to high interaction energy. As soon as these sites become occupied, sorption occurs on the less active site and gives rise to lower heat of sorption. At low-moisture content the higher heat of sorption could be due to strong interaction between water molecules and hydrophilic groups of chitosan.

Effect of plasticizer on moisture content

The addition of the plasticizing agent to edible film is required to overcome film brittleness, which is caused by extensive intermolecular forces. Plasticizers reduce these forces, thereby improving flexibility and extensibility of the films.[44] Since, plasticizers extend, dilute and soften the structure effectively, the chain mobility is increased and hence water vapor permeates with enhanced rate.

In the current work, different plasticizers, namely, glycerol, sucrose, and carbitol, were added to plain chitosan solution (in 40% weight of dry chitosan) and the WVP of resulting films was investigated at RH of 100% at 25°C. The results, as depicted in

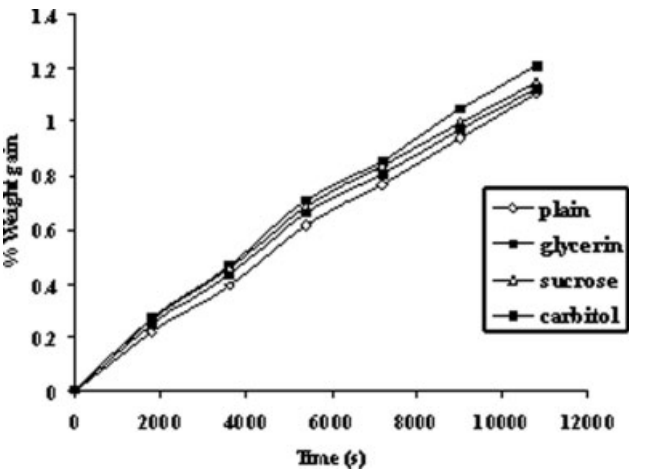

Figure 10 Kinetics of permeation of water vapor through plasticized films.

Figure 10, clearly indicate that the amount of moisture which permeates through the films, increases due to addition of plasticizer. However, this effect is almost negligible in the case of carbitol-loaded film. The enhancement in water vapor permeation follows the order carbitol < sucrose < glycerol. Thus, carbitol seems to be the most appropriate plasticizer as its presence results in minimum enhancement in permeation of water vapors when compared with other plasticizers. This may probably be due to the fact that carbitol has ability to bind with less water vapor molecules than other plasticizers used, and so it provides lowest WVP. The same finding has also been reported by McHugh et al.[45] The structural modification of chitosan network by plasticizers and their hydrophilic nature are the main reasons for enhancement in WVP. The WVTR, as determined for carbitol, sucrose and glycerol were found to be 0.240, 0.260, and 0.265, respectively. Therefore, it can be concluded that due to the addition of plasticizer, vapor permeability is observed to increase and carbitol provides minimum water vapor permeation.

Isotherm for plain chitosan and ZOLC films

The entrapment of ZnO nanoparticles into chitosan film is expected to cause change in vapor permeability of the film. To investigate this, the equilibrium moisture content of PC film and ZOLC(2) films were determined at different water activities and are depicted in Figure 11. It is clear that for a given water activity nano zinc oxide-loaded film exhibits less moisture uptake. This may simply be explained on the basis of the fact that the presence of zinc oxide metal nanoparticles reduces the overall hydrophilic character of the film. It has been reported on the basis of the measurement of the relative contact angle and activity ratio that ZnO nanoparticles exhibit excellent hydrophobic nature.[46] We also measured percent moisture content permeated through PC and ZOLC films at different time intervals (see

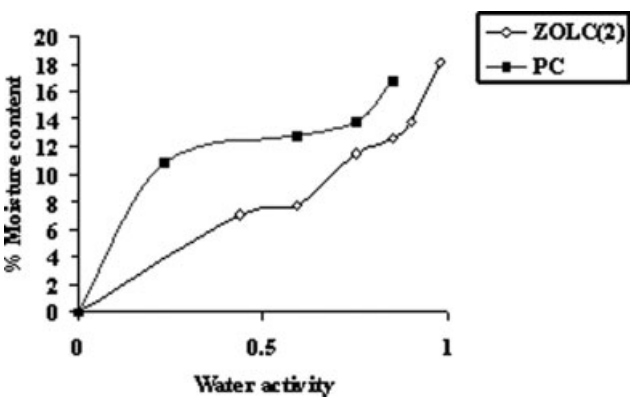

Figure 11 Isotherm for PC and ZOLC(2) films at 25°C.

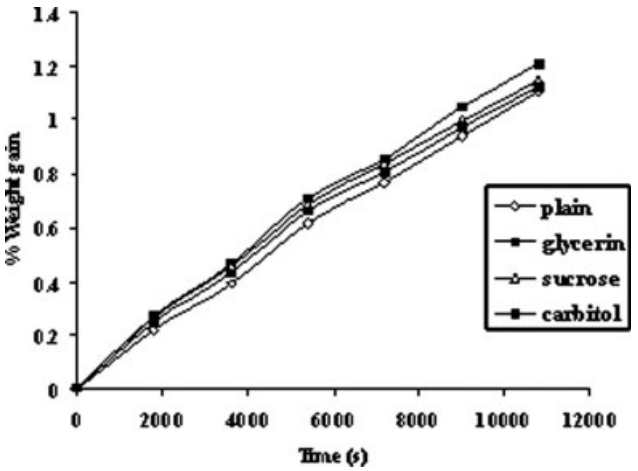

Figure 12 Kinetics of water vapor permeation through plain and ZOLC(2) films at 25°C.

Fig. 12) and determined related parameters. The observed lower parameter values for ZOLC film may be attributed to the hydrophobic nature of ZnO nanoparticles as discussed above. In addition, there are possibilities of H-bonding interactions between ZnO nanoparticles and —OH groups present in chitosan chains within the film. This argument is supported by the work done by Yang et al.,[47] who have reported hydrogen bonding interactions between ZnO and carboxylic and amino groups of enzyme molecules. These hydrogen bonding interactions may produce additional crosslinks within the film network and hence discourage the diffusion of water vapors through films. The WVTR, WVP for the plain, and nano ZnO-loaded films were found to be 17.5×10^{-2}, 55.9×10^{-11}, and 15.7×10^{-2} g m^{-2} s^{-1}, 50.3×10^{-11} g m^{-1} s^{-1} Pa^{-1}, respectively. The relatively lower values obtained for ZOLC film also support our findings.

Antibacterial activity of PC and ZOLC films

The antibacterial activity of ZOLC film was investigated using *E. coli* 11,634 as model bacteria by zone inhibition and cell count methods.[48] The results of zone inhibition method, as depicted in Figure 13, clearly indicate that the Petri plate supplemented with ZnO-loaded film shows a clear zone of inhibition around the piece of film (see Fig. 14), whereas a dense population is observed in the petri-plate containg PC film. This indicates that ZnO nanoparticles demonstrate fair antibacterial action against *E. coli*. In addition, the biocidal action seems more effective in the petri-plate that contain ZOLC(4) film as compared with ZOLC(2) film that may simply be due to the fact that ZOLC(4) contains higher concentration of ZnO nanoparticles. Here, it is also noteworthy to mention that chitosan has a very fair reputation as

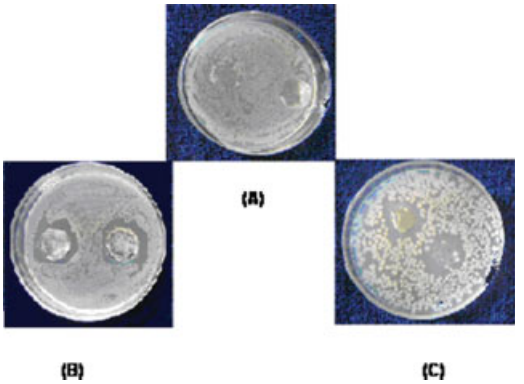

Figure 13 Evaluation of antibacterial action for (A) PC, (B) ZOLC(2), and (C) ZOLC(4) films by "zone inhibition" method. [Color figure can be viewed in the online issue, which is available at www.interscience.wiley.com.]

antibacterial agent,[49] but in the present study, it did not show any biocidal action as can be seen in Figure 13 (see Petri plate with plain chitosan film, taken as control). This may be explained on the basis of the fact that a high molecular weight chitosan (i.e., 1.42×10^6) has been used in the preparation of films, and so it has almost been ineffective against bacterial growth.[50] In addition, the kinetics of bacterial killing was also investigated (see Fig. 14). It is quite clear that there is an appreciable growth rate of bacteria in the control set while the growth rate is suppressed to a greater extent in the solution containing the zinc oxide-loaded film. Both of these experiments reveal that nano ZnO has great potential to be used in edible films as antimicrobial agent. Finally, Figure 15 depicts the growth of bacterial colonies produced in the petri-plates supplemented with uniformly distributed small pieces of plain, ZOLC(2), and ZOLC(4) films. The number of colonies present was found to be 1976 and 1504, respectively. It is clear that the number of colonies decreases with increase in ZnO content. The mechanism of antibacterial action of nano ZnO has already been reported in the literature. According to current research reports on mechanism of antibacterial action of ZnO nanoparticles, it is believed that nano ZnO, on coming in contact with bacterial cells in the presence of moisture produce reactive oxygen species such as hydroxyl radicals, superoxides, and H_2O_2.[24] Since, the hydroxyl radicals and super oxides are negatively charged particles; they cannot penetrate into the cell membrane and must remain in direct contact with the outer surface of bacteria and cause severe damage to proteins, lipids, and DNA.[51] However, H_2O_2 penetrates the cell membrane and kills the bacteria.[52]

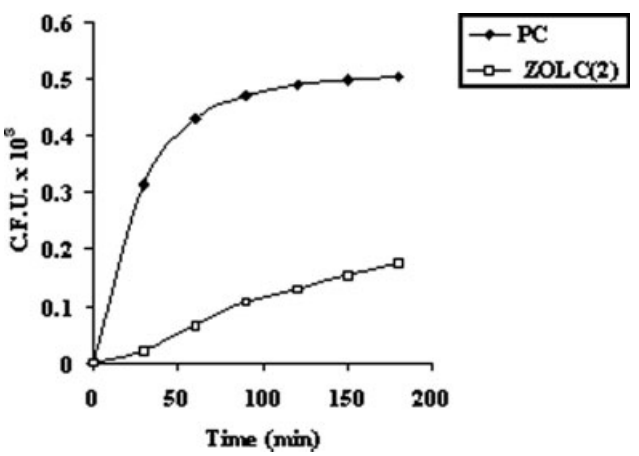

Figure 14 Kinetics of bacterial growth for PC and ZOLC(2) films against *E. coli*.

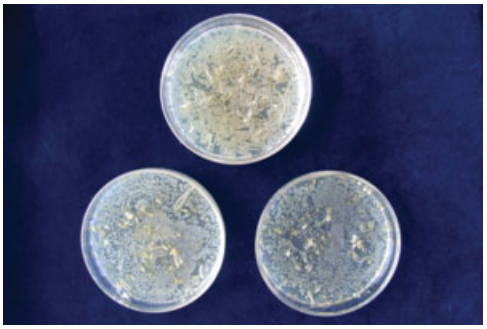

Figure 15 Number of colonies grown in petri-plates supplemented with (A) PC, (B) ZOLC(2), and (C) ZOLC(4) films. [Color figure can be viewed in the online issue, which is available at www.interscience.wiley.com.]

Here, it is also worth mentioning that formation of inhibition zone around the zinc oxide nanoparticles-loaded films also indicates that ZnO nanoparticles must have diffused away from the film, thus causing bacterial cells death and forming clear zone of inhibition around the circular film. This means that if food stuff is wrapped by the film then ZnO nanoparticles shall diffuse into the food stuff and attack the growing bacteria. As stated in the Introduction section, zinc is also used as nutrient and therefore ZnO nanoparticles that diffuse from the film into the food stuff shall not produce any harmful effect on the health of the user.

CONCLUSIONS

From the above study, it is concluded that moisture uptake of chitosan films decreases with increase in the temperature, whereas WVP shows just opposite trend. The GAB isotherm successfully interprates the moisture uptake data. The presence of plastisizer enhances the WVP. However, the zinc oxide nanoparticles-loaded film exhibits less moisture uptake as compared with PC film. The nano ZnO-loaded film exhibit excellent antibacterial action against *E. coli*.

References

1. Burt, S. J Food Microbiol 2004, 94, 223.
2. Conte, A.; Sinigaglia, M.; Del Nobile, M. A. J Food Prot 2006, 90, 861.
3. Moller, H.; Grelier, S.; Pardon, P.; Coma, V. J Agric Food Chem 2004, 52, 6585.
4. Khallofufi, S.; Giasson, J.; Ratti, C. Can Agric Eng 2000, 42, 7.1
5. Cagri, A.; Ustunol, Z.; Ryser, E. T. J Food Prot 2004, 68, 833.
6. Vargas, M.; Albors, A.; Chiratt, A.; Gongalezmartinez, C. Food Hydrocolloids 2009, 23, 536.
7. The, D. P.han; Debeaufort, F.; Voilley, A.; Luu, D. J Food Eng 2009, 90, 548.
8. Bourtoom, T.; Chinnan, M. S. LWT Food Sci Technol 2008, 41, 1633.
9. Bertuzzi, M. A.; Castro Vidaurre, E. F.; Armada, M.; Gottifredi, J. C. J Food Eng 2007, 80, 972.
10. Perez-Mateas, M.; Montero, P.; Gomez-Guillen, M. C. Food Hydrocolloids 2009, 23, 53.
11. Sivarooban, T.; Hettiarachchy, N. S.; Johnson, M. G. Food Res Int 2008, 41, 781.
12. Del Nobile, M. A.; Conte, A.; Incoronato, A. L.; Panza, O. J Food Eng 2008, 98, 57.
13. Suppakul, P.; Miltza, J.; Sonneveld, K.; Bigger, S. W. J Food Sci 2003, 68, 408.
14. Eswaranandam, S.; Hettiarachychy, N. S.; Johnson, M. G. J Food Sci 2004, 69, 79.
15. Chaibi, A.; Ababouch, L. H.; Belasri, K.; Boucetta, S.; Busta, F. F. Food Microbiol 1997, 14, 161.
16. Kim, H.; Roh, I.; Kim, K.; Jang, I.; Ha, s; Song, K.; Park, S.; Lee, W.; Youn, K.; Bae, D. J Microbiol Biotechnol 2006, 16, 597.
17. Gucbilmez, C. M.; Yemenicioglu, A.; Arslanoglu, A. Food Res Int 2007, 40, 80.
18. Conte, A.; Serpanza, B.; Sinigaglia, M.; Del Nobbile, M. A. J Food Prot 2007, 70, 114.
19. Singh, M.; Singh, S.; Prasad, S.; Gambhir, I. S. Digest J Nanometer Biostruct 2008, 3, 115.
20. Sondi, I.; Salopek–Sondi, B. J Colloids Interface Sci 2004, 275, 177.
21. Yadav, A.; Prasad, V.; Kathe, A. A.; Raj, S.; Yadav, D.; Sundarmoorthy, C.; Vigneshvaran, N. Bull Mater Sci 2006, 29, 641.
22. Jones, N.; Ray, B.; Ranjit, K. T.; Manna, A. C. FEMS Microbiol Lett 2007, 279, 71.
23. Tam, K. H.; Djurisic, A. B.; Chan, C. M. N.; Xi, Y. Y.; Tse, C. W.; Leung, Y. H.; Chan, W. K.; Leung, F. C. C. Thin Solid Films 2008, 516, 6167.
24. Padmawathy, N.; Vijayaraghavan, R. Sci Technol Adv Mater 2008, 9, 1.
25. Shi, L.; Zhou, J.; Gunasekaran, S. Mater Lett 2008, 62, 4383.
26. Guilbal, E.; Saucedo, I.; Jansson-Charrier, M.; Delanhge, B.; Le-Cloirec, P. Water Sci Technol 1994, 30, 183.
27. Coma, V.; Martial-Gros, A.; Garreau, S.; Copienet, A.; Salin, F.; Deschamps, A. J Food Sci 2002, 67, 1162.
28. Alhamdan, A. M.; Hassan, B. H. J Food Eng 1999, 39, 301.
29. Oluwamukomi, M. O.; Adeyemi, I. A.; Odeyemi, O. O. Agric Eng Int 2008, 10, 1.
30. ASTM Standard Test Method for Water Vapour Transmission of Materials (E 96-93), 1993, p 701.
31. Bozdemir, O. A.; Tutas, M. J Chem 2003, 27, 773.
32. Qin, Y.; Zhu, C.; Chen, Y.; Zhang, C. J Appl Polym Sci 2006, 101, 766.
33. Pal, S.; Tak, Y. K.; Song, J. M. Appl Environ Microbiol 2007, 73, 1720.
34. Thomas, V.; Bajpai, S. K.; Mohan, Y. M.; Sreedhar, B. J Colloid Interf Sci 2007, 315, 389.
35. Vigneshwaran, N.; Kumar, S.; Kathe, A. A.; Varadrajan, P. V.; Prasad, V. Nanotechnology 2006, 17, 5087.
36. Li, C.; Li, Y.; Luo, L.; Fu, M.; Chil, J. Chem Soc 2008, 53, 1615.
37. Zhong, Q.; Xia, W. Food Technol Biottechnol 2008, 46, 262.
38. Wu, Z. Y.; Cai, J. H.; Ni, G. Thin Solid Films 2008, 516, 7318.
39. Abramovic, H.; Klofutar, C. Acta Chim Solv 2002, 49, 835.
40. Hassan, B. H. J King Soud Univ Agric Sci 2002, 14, 105.
41. Al-Muhtaseb, A. H.; Mcminn, W. A. M.; Mage, T. R. A. Food Bioproducts Process 2002, 80, 118.
42. Hagenmaier, R. D.; Shaw, P. E. J Agric Food Chem 1996, 38, 1799.
43. Napierala, D. M.; Nowotarska, A. Acta Agrophys 2006, 7, 151.
44. Forssel, P.; Lahtinen, R.; Lahenin, M.; Myllarimen, P. Carbohydr Polym 2002, 47, 125.
45. Mchugh, T. H.; Bustillos, R. A.; Krochta, J. M. J. Agric Food Chem 1994, 42, 899.
46. Tang, L.; Zhou, B.; Sun, F.; Li, Y.; Wang, Z. Chem Eng J 2008, 139, 642.
47. Yang, Y. H.; Yang, M. H.; Jiang, J. H.; Shen, G. L.; Yu, R. Q. Chin Chem Lett 2005, 16, 951.
48. Bajpai, M.; Bajpai, S. K.; Gupta, P.; Ali, E. J Cotton Sci 2008, 12, 280.
49. Materji, N. V. React Funct Polym 2000, 46, 1.
50. Li, X.; Feng, X.; Yang, S.; Wang, T. Iran Polym J 2008, 17, 843.
51. Kohen, R.; Nyska, A. Tox Pathol 2002, 6, 620.
52. Fang, M.; Chen, J. H.; Xu, X. L.; Yang, P. H.; Hildebrand, H. F. Int J Antimicrob Agents 2006, 26, 513.